

On the dynamics of a thin elastica

H. Sheheitli ^{a,*}, R.H. Rand ^{a,b}

^a Department of Mechanical and Aerospace Engineering, Cornell University, Ithaca, NY, USA

^b Department of Mathematics, Cornell University, Ithaca, NY, USA

ARTICLE INFO

Article history:

Received 15 October 2011

Received in revised form

5 February 2012

Accepted 15 March 2012

Available online 23 March 2012

Keywords:

Elastica

Non-local modes

DPM

Method of direct partition of motion

WKB method

Bifurcation

ABSTRACT

We revisit the two degrees of freedom model of the thin elastica presented by Cusumano and Moon (1995) [3]. We observe that for the corresponding experimental system (Cusumano and Moon, 1995 [3]), the ratio of the two natural frequencies of the system was ≈ 44 which can be considered to be of $O(1/\varepsilon)$, where $\varepsilon \ll 1$. The presence of such a vast difference between the frequencies motivates the study of the system using the method of direct partition of motion (DPM), in conjunction with a rescaling of fast time in a manner that is inspired by the WKB method, similar to what was done in Sheheitli and Rand (to appear) [8]. Using this procedure, we obtain an approximate expression for the solutions corresponding to non-local modes of the type observed in the experiments (Cusumano and Moon, 1995 [2]). In addition, we show that these non-local modes will exist for energy values larger than a critical energy value that is expressed in terms of the parameters. The formal approximate solution is validated by comparison with numerical integration.

© 2012 Elsevier Ltd. All rights reserved.

1. Introduction

Mechanical systems subjected to high-frequency parametric excitation are known to exhibit qualitative changes in their dynamical properties such as natural frequencies, the number and stability of equilibrium points, and bifurcation paths [1,4,9,10]. The method of direct partition of motion (DPM) [1] was developed particularly for the study of such non-autonomous problems. Recently, it was shown that DPM can also be useful for the study of autonomous multi-degree of freedom systems possessing vastly different frequencies [7,8]. While the averaging method has been previously used to analyze systems with vastly different frequencies [5,11], it is illustrated in [8] that DPM, when combined with a rescaling of fast time as inspired by the WKB method [12], allows the study of solutions in which the fast degree of freedom is strongly influenced by the slow one. That is, in the cases where the averaging method is used, the slow variable has an $O(\varepsilon)$ effect on the fast variable, whereas in [8] the fast variable is to leading order expressed explicitly in terms of the slow variable.

In this work, we revisit the problem of the thin elastica studied by Cusumano and Moon [3], who presented a two degree of freedom model, representing the first bending and first torsional modes of the elastica. The model was shown to capture much of the behavior observed in the experiments such as loss of planar stability and the

existence of non-local modes [3]. A variety of perturbation methods were used to study the elastica model [6], however, that analysis required that the coupling parameter to be of $O(\varepsilon)$. This does not apply to the experimental system [3] in which the coupling parameter was ≈ 1.74 which is rather of $O(1)$. The experimental system also had a ratio of frequencies ≈ 44 which can be considered to be of $O(1/\varepsilon)$, where $\varepsilon \ll 1$. This latter observation implies that the system is best viewed as one with vastly different frequencies and that DPM can be useful for understanding its dynamics. Also, the fact that the coupling is $O(1)$ allows the slow variable to appear in the leading order dynamics of the fast variable, which appears as a fast oscillator with a slowly varying frequency. This suggests the use of a rescaling of fast time in a manner that is inspired by the WKB method, as illustrated in [8].

In Section 2, we present the two degree of freedom model of the thin elastica and illustrate the non-local modes that it exhibits. In Section 3, we present the form of the assumed solution and the end results of the DPM procedure which consist of an equation governing the leading order dynamics of the slow variable (the bending mode), as well as an expression of the fast variable (the torsional mode) in terms of the slow variable. We also discuss the special solutions corresponding to the non-local modes and present an expression for the critical energy value above which these solutions exist. Finally, in Section 4, we validate the approximate solution by comparing it to that from numerical integration. The procedure for obtaining the approximate solution is detailed in Appendices A and B, while Appendix C explains how we obtain the expression for the non-local modes and the critical energy value in terms of the parameters.

* Corresponding author. Tel.: +1 6072275728.

E-mail addresses: hs497@cornell.edu (H. Sheheitli), rhr2@cornell.edu (R.H. Rand).

2. The two degree of freedom elastica model

The derivation of the model studied in this work was presented in detail in [3]. We present the following summary of [3] for the convenience of the reader. The analysis starts with the equations for an inextensible, unshearable, prismatic, linearly elastic rod with the additional constraint that one of the curvature components is zero. For simplicity, the theory was then reduced to the lowest order in the displacements which are assumed to be much smaller than unity. This implies that although two of the Euler angles are first order in the displacements, the torsional rotation need not be small. Also, in the experiments described in [2], the torsional motions of the elastica appeared to be close to the first torsional mode. Based on these assumptions, the displacements in the plane of the cross-section of the rod were transformed into polar coordinates consisting of a generalized displacement and the torsional angle. Finally, the assumed-modes method was employed to reduce the system of partial differential equations governing the generalized displacement and the torsional angle into a system of ordinary differential equations governing the time evolution of the amplitudes of the generalized displacement (representing the first generalized bending mode) and the first torsional mode. Ignoring dissipation and external forcing, the latter two degree of freedom system modeling the elastica can be expressed as [3]

$$\ddot{y} + y - \gamma \dot{x}^2 y = 0$$

$$(\mu + \gamma y^2) \ddot{x} + \mu \Omega^2 x + 2\gamma y \dot{y} \dot{x} = 0 \tag{1}$$

where y and x represent the first bending and torsional mode, respectively. μ is a dimensionless parameter related to the moment of inertia, γ is a coupling parameter and Ω is the ratio of the dimensionless natural frequencies of the two modes. In [3], it was shown numerically that this conservative system possesses

two symmetric families of non-linear modes with a frequency-amplitude characteristic similar to that observed in the experiments. The aim of the work here is to gain insight on the emergence of these non-local modes in the conservative problem and to obtain approximate analytic expressions for these modes.

The conserved energy of the system can be expressed as

$$h = \frac{1}{2}(\mu + \gamma y^2)\dot{x}^2 + \frac{1}{2}\dot{y}^2 + \frac{1}{2}(\mu\Omega^2 x^2 + y^2) \tag{2}$$

To illustrate the bifurcation that occurs as energy is increased, giving rise to the non-local modes, we will numerically integrate the system in Eqs. (1) with parameter values that match those reported in the experimental setup [3]:

$$\gamma = 1.74, \quad \mu = 0.0113, \quad \Omega = 44$$

We will choose a value of the energy h and take initial conditions of the form

$$\begin{cases} y(0) = b, & x(0) = \sqrt{\frac{(2h - b^2)}{\mu\Omega^2}} \\ \dot{y}(0) = 0, & \dot{x}(0) = 0 \end{cases}$$

Fig. 1 shows the torsional mode variable, x , which is typically a fast oscillation with a slowly modulated amplitude. Fig. 2a shows the oscillation of the bending mode variable, y , typical of low enough energies. As the energy is slightly increased, we can see y undergoing a non-local oscillation having a non-zero mean value, as in Fig. 2b. With a careful choice of initial amplitudes, y appears to be almost fixed about a non-zero value as shown in Fig. 3. The latter oscillation corresponds to a non-local mode that arises as the energy increases past a critical value. Still, for a large enough initial amplitude, oscillations about the origin are possible, as illustrated in Fig. 4. The bifurcation that gives rise to the non-local modes corresponds to a pitchfork bifurcation in a Poincare map of

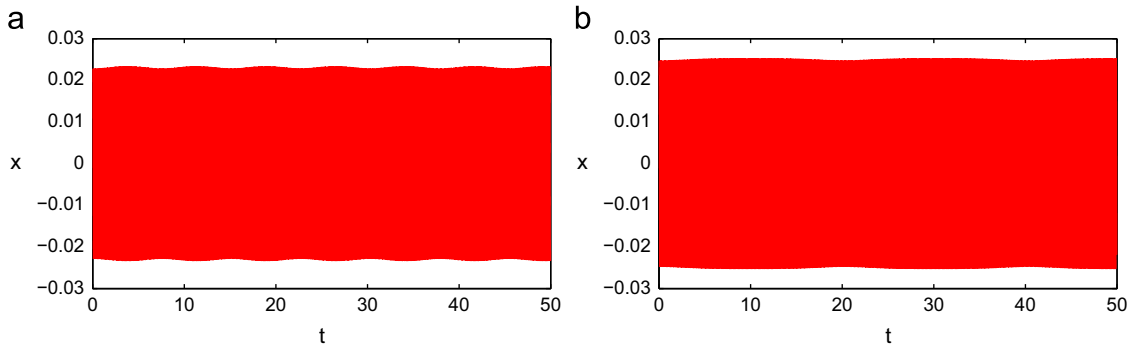


Fig. 1. Plot of x vs. time for the initial conditions with: (a) $h = 0.006$, $b = 0.025$, (b) $h = 0.007$, $b = 0.025$.

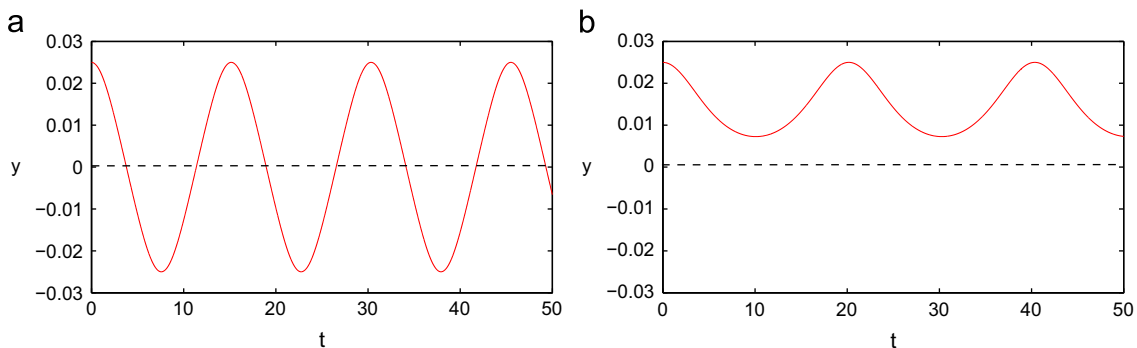


Fig. 2. Plot of y vs. time for the initial conditions with: (a) $h = 0.006$, $b = 0.025$, (b) $h = 0.007$, $b = 0.025$.

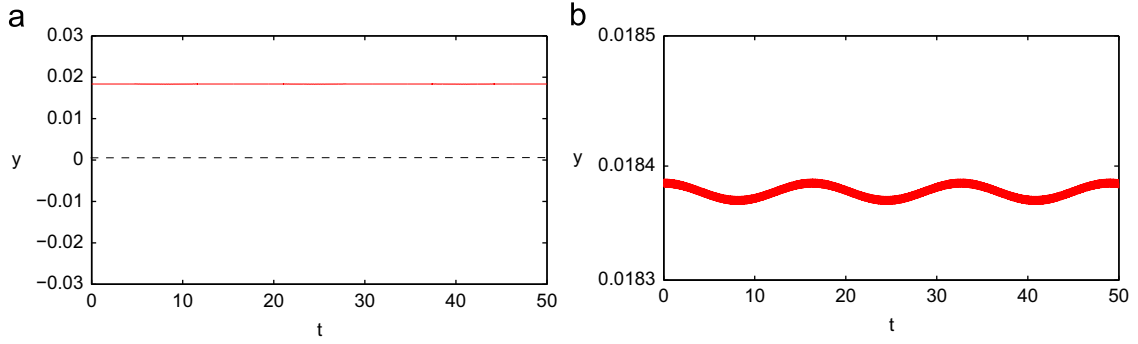


Fig. 3. Plot of y vs. time for the initial conditions with: (a) $h = 0.007$, $b = 0.0184$, (b) zoom in on the solution.

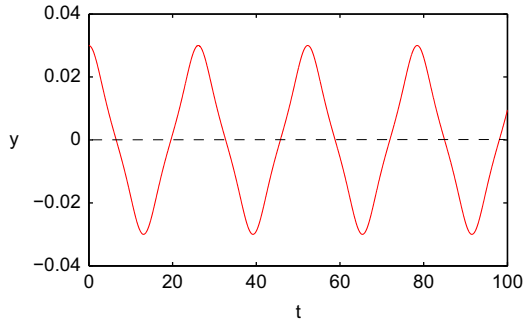


Fig. 4. Plot of y vs. time for the initial conditions with $h = 0.007$, $b = 0.03$.

the system, as illustrated in Fig. 5. As energy increases past a critical value, the fixed point of the map, corresponding to the torsional mode with $y=0$, loses stability and two new centers are born corresponding to two non-local modes. Closed orbits about each of these centers correspond to solutions of the type illustrated in Fig. 2b, while the large orbits engulfing both centers correspond to oscillations about the origin as in Fig. 4.

The aim of the paper is to explain the dependence of the solution on initial conditions and the parameters of the system. We will also obtain an expression for the critical energy value at which the bifurcation occurs and an approximate expression for the non-local modes it gives rise to.

3. The approximate solution

For the system studied experimentally in [3], $\Omega \approx 44$, so we will assume that

$$\Omega = \frac{1}{\varepsilon}, \quad \varepsilon \ll 1$$

Also, we rescale x so that

$$x = \chi \sqrt{\frac{\varepsilon}{\gamma}} \quad \text{where } \chi = O(1)$$

Then, the system in Eqs. (1) becomes

$$\ddot{y} + y - \varepsilon \dot{\chi}^2 y = 0$$

$$(1 + \kappa y^2) \ddot{\chi} + \frac{1}{\varepsilon^2} \dot{\chi}^2 + 2\kappa y \dot{y} \dot{\chi} = 0 \quad (3)$$

where we have divided the x equation by μ and defined a new parameter $\kappa = \gamma/\mu$. The corresponding energy expression is

$$h = \frac{1}{2} \left(\frac{1}{\kappa} + y^2 \right) \varepsilon \dot{\chi}^2 + \frac{1}{2} \dot{y}^2 + \frac{1}{2} \left(\frac{1}{\varepsilon \kappa} \chi^2 + y^2 \right) \quad (4)$$

Applying the strategy first illustrated in [8], we will look for a solution of the form suggested by DPM and WKB:

$$\chi = \chi(\zeta, T), \quad y = y_0(\zeta) + \varepsilon y_1(\zeta, T)$$

$$\text{where } \zeta = t \quad \text{and} \quad \frac{dT}{dt} = \frac{\omega(\zeta)}{\varepsilon}, \quad \omega(\zeta) = \omega_0(\zeta) + \varepsilon \omega_1(\zeta) + \dots \quad (5)$$

At the end of the DPM procedure detailed in Appendix B, we obtain the following equation governing the leading order slow dynamics:

$$\frac{d^2 y_0}{dt^2} + y_0 - y_0 \frac{C^2}{2\varepsilon} (1 + \kappa y_0^2)^{-3/2} = 0 \quad (6)$$

We assume initial conditions of the form as

$$\begin{cases} y(0) = b \\ x(0) = \chi(0) \sqrt{\frac{\varepsilon}{\gamma}} = a \sqrt{\frac{\varepsilon}{\gamma}} \end{cases} \rightarrow \begin{cases} y_0(0) \approx b \\ \chi(0) = a \end{cases}$$

then the constant appearing in Eq. (6) can be related to the initial amplitudes by the following relation:

$$C^2 = \gamma a^2 \sqrt{1 + \kappa b^2}$$

In Appendix A, we show that the fast variable χ can be expressed in terms of the slow variable y_0 as

$$\chi \approx C \sqrt{\omega_0(\zeta)} \cos T$$

$$\text{with } \omega_0 = (1 + \kappa y_0^2)^{-1/2} \quad (7)$$

Also, the fast component of y is found to be

$$y_1 \approx y_0 \omega_0 \frac{C^2}{8} \cos 2T$$

Knowing the initial amplitudes a and b , we solve for the corresponding value of C , then we plot the phase portrait and pick out the orbit corresponding to $y_0(0) = b$, $\dot{y}_0(0) = 0$. This latter orbit will correspond approximately to the leading order slow oscillation of the bending variable y , so this allows us to tell what type of solution the full system will have. The arrows in Fig. 6a–c point to the orbits corresponding to the solutions in Figs. 2a, b and 4, respectively. Fig. 7 shows the phase plane for the y_0 equation with the value of C corresponding to the initial conditions that led to the non-local mode shown in Fig. 3. We can see that one of the centers is $(y_0 = 0.0184, \dot{y}_0 = 0)$, then the orbit corresponding to $y_0(0) = b = 0.0184, \dot{y}_0(0) = 0$ is the fixed point itself. In Appendix C, we show that for each energy value satisfying the following condition:

$$h > h_{cr} = \frac{1}{\kappa} \quad (8)$$

there exists an initial amplitude b^* that will lead to a value of C such that the y_0 equation has a fixed point with $y_0 = b^*$; such initial

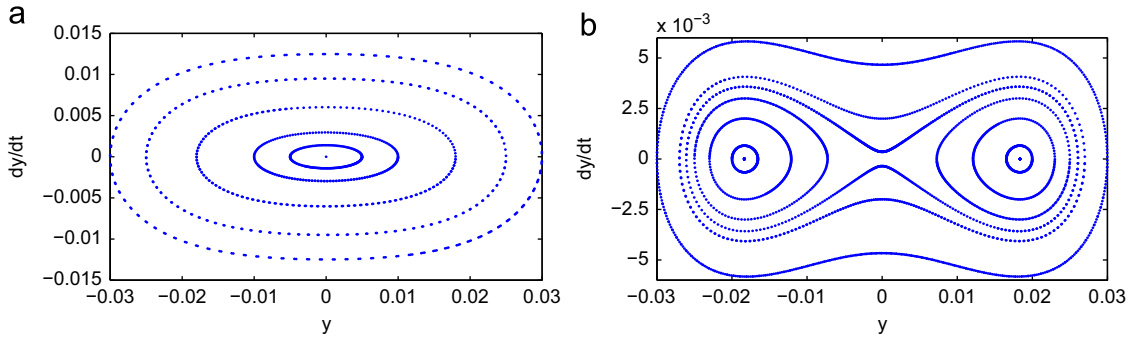


Fig. 5. Plot of a Poincaré map ($x=0, \dot{x} > 0$) for (a) $h=0.006$, (b) $h=0.007$.

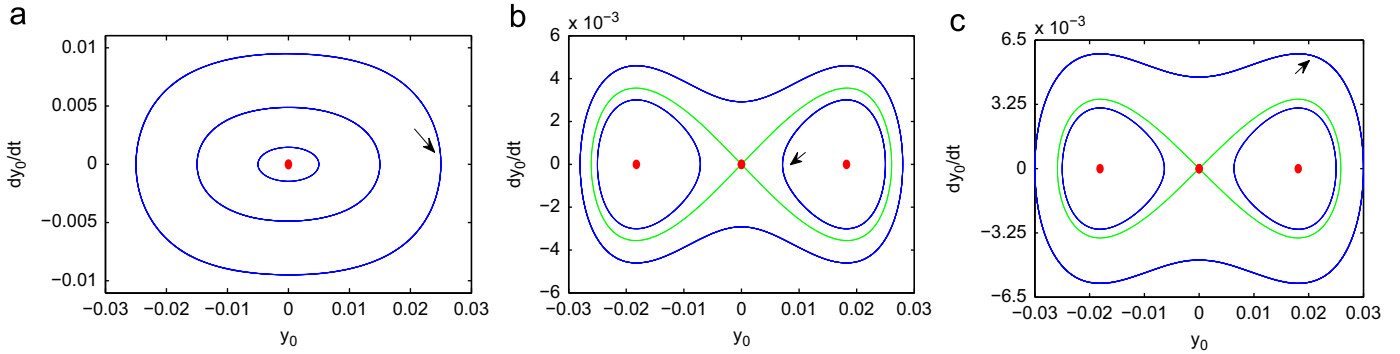


Fig. 6. Phase plane for the y_0 equation (a) $h=0.006$, $b=0.025$; $C=0.2042$, (b) $h=0.007$, $b=0.025$; $C=0.2213$, (c) $h=0.007$, $b=0.03$; $C=0.2203$.

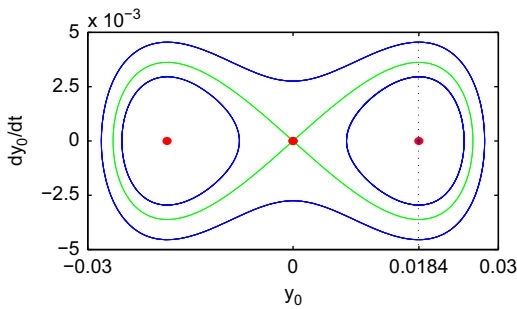


Fig. 7. Phase plane for the y_0 equation for $h=0.007$, $b=0.0184$; $C=0.2215$.

conditions will lead to the non-local modes. As explained in Appendix C, b^* is found to be

$$b^* = \sqrt{\frac{2}{3} \left(h - \frac{1}{\kappa} \right)} \tag{9}$$

In other words, for a fixed energy level, the following initial conditions:

$$\begin{cases} y(0) = b^* = \sqrt{\frac{2}{3} \left(h - \frac{1}{\kappa} \right)}, & x(0) = a^* = \sqrt{\varepsilon \kappa (2h - b^{*2})} \\ \dot{y}(0) = 0, & \dot{x}(0) = 0 \end{cases} \tag{10}$$

will lead to non-local modes in which

$$y_0 \approx b^* \quad \text{and} \quad \chi \approx a^* \cos\left(\frac{\omega^*}{\varepsilon} t\right)$$

$$\text{So that } y \approx b^* + \varepsilon \frac{a^{*2} b^*}{8} \cos\left(2 \frac{\omega^*}{\varepsilon} t\right) \quad \text{and} \quad x \approx \sqrt{\frac{\varepsilon}{\gamma}} a^* \cos\left(\frac{\omega^*}{\varepsilon} t\right) \tag{11}$$

$$\text{where } \omega^* = (1 + \kappa b^{*2})^{-1/2} \tag{12}$$

The expression for the non-local mode solution shows that the bending variable will have a frequency that is twice that of the torsional one, which is consistent with what was observed in [3].

4. Validation

Taking the same parameter values as in Section 2, we choose a value of $h=0.05$ and compare the approximate solution obtained from numerical integration of the y_0 equation to that of the full system. Figs. 8 and 9 show plots of y vs. time and x vs. time, respectively, for three different initial conditions. The approximate solution is represented by a dashed line, while the numerical solution of the full system is represented by a solid line. It is hard to distinguish the two solutions as they almost completely overlap, this illustrates that the two solutions agree well. In Appendix D, we present more comparison plots of solutions for different energy values as well as for a larger γ value. The error in the approximate solution becomes more visible for larger values of energy far from the bifurcation value. In [3], the frequency amplitude characteristics of the non-linear modes were obtained numerically and presented as a plot of frequency vs. amplitude of the torsional variable, as well as frequency vs. energy. Here, we have obtained approximate analytic expressions for the frequency and amplitude of y for the non-local mode solutions, as a function of the energy value and the parameters. Fig. 10 shows the frequency amplitude characteristic curves that we obtain using Eqs. (10)–(12). The two plots match very well with those presented in [3].

5. Conclusion

The method of direct partition of motion was used to study the dynamics of the thin elastica model presented in [3]. This was

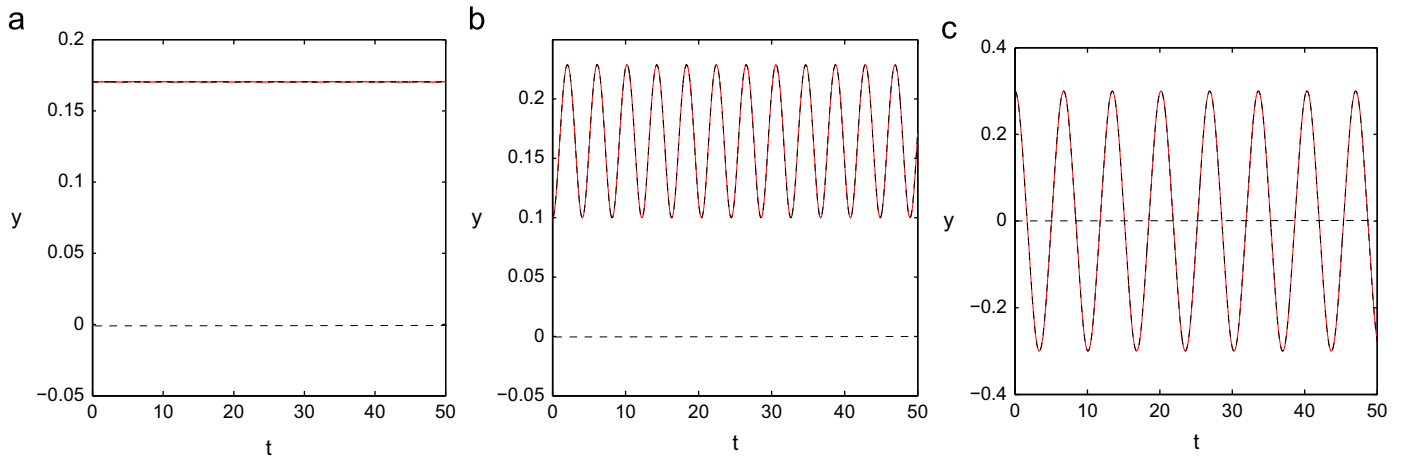


Fig. 8. y vs. time for (a) $h=0.05, b=0.1703$, (b) $h=0.05, b=0.1$ (c) $h=0.05, b=0.3$.

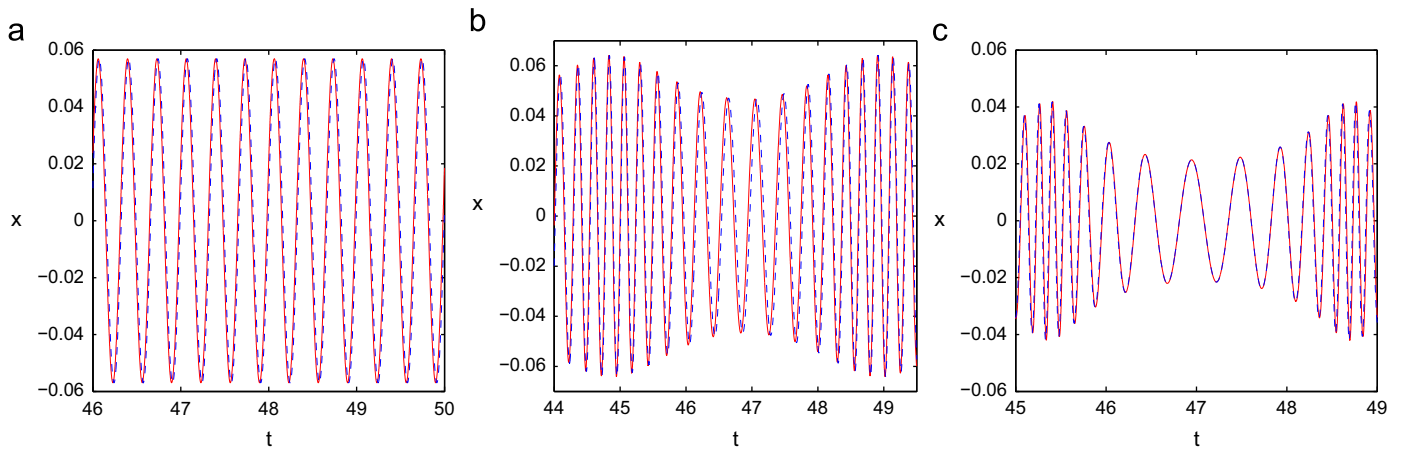


Fig. 9. x vs. time for (a) $h=0.05, b=0.1703$, (b) $h=0.05, b=0.1$ (c) $h=0.05, b=0.3$.

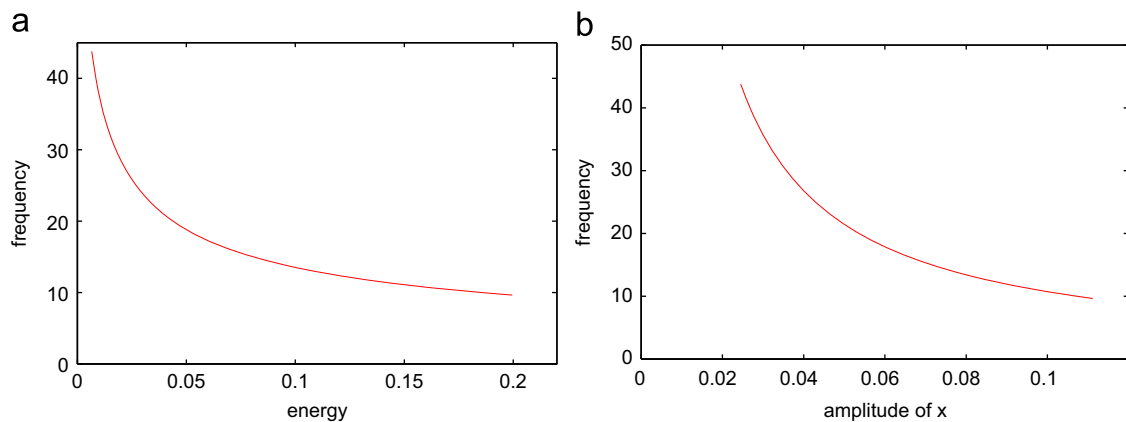


Fig. 10. Frequency amplitude characteristics for the non-local mode solution (a) frequency vs. energy value and (b) frequency vs. amplitude of the torsional variable x .

based on the observation that the frequency ratio for the experimental setup was of $O(1/\epsilon)$ and so the system is best viewed as one with vastly different frequencies. It was also observed that the coupling parameter value corresponding to the experimental setup was $O(1)$ such that the slow variable affects the leading order dynamics of the fast variable; this required the treatment of the fast variable as an oscillator with a slowly varying frequency and thus using a rescaling of fast time inspired by the

WKB method. The procedure leads to an approximate expression for the non-local modes, as well as the critical energy value at which they arise, in terms of the parameters of the system. The results are checked by comparison to numerical integration and found to agree well. Finally, we note that the proposed procedure has proven useful for the study of conservative systems. The attempt to extend it to the study of the dynamics in the presence of damping or forcing is left for future work.

Appendix A. The WKB solution for the fast degree of freedom

The assumed solution has the following form:

$$\chi = \chi(\xi, T), \quad y = y_0(\xi) + \varepsilon y_1(\xi, T)$$

where $\xi = t$ and $\frac{dT}{d\xi} = \frac{\omega(\xi)}{\varepsilon}$, $\omega(\xi) = \omega_0(\xi) + \varepsilon \omega_1(\xi) + \dots$ (13)

Here, we are stretching the new fast timescale to accommodate for the cubic order term, $2\kappa y \dot{y}$, that is present in the equation of the fast oscillator.

We plug the expression for the solution into Eqs. (3); multiplying the χ equation by ε^2 , we get

$$\omega_0^2(1 + \kappa y_0^2) \frac{\partial^2 \chi}{\partial T^2} + \chi + \varepsilon \left[2\kappa \omega_0^2 \left(y_0 \frac{\partial y_1}{\partial T} \frac{\partial \chi}{\partial T} + y_0 y_1 \frac{\partial^2 \chi}{\partial T^2} \right) + 2\kappa \omega_0 y_0 \frac{dy_0}{d\xi} \frac{\partial \chi}{\partial T} \right. \\ \left. + (1 + \kappa y_0^2) \left(2\omega_0 \frac{\partial^2 \chi}{\partial \xi \partial T} + \frac{d\omega_0}{d\xi} \frac{\partial \chi}{\partial T} + 2\omega_0 \omega_1 \frac{\partial^2 \chi}{\partial T^2} \right) \right] = 0 \quad (14)$$

As in the WKB method [12], we ought to choose ω_0 , so that the χ equation takes the form

$$\frac{\partial^2 \chi}{\partial T^2} + \chi + O(\varepsilon) = 0$$

This results in the following expression for ω_0 :

$$\omega_0 = (1 + \kappa y_0^2)^{-1/2} \quad (15)$$

The equation governing χ then becomes

$$\frac{\partial^2 \chi}{\partial T^2} + \chi + \varepsilon \left[2\kappa \omega_0^2 \left(y_0 \frac{\partial y_1}{\partial T} \frac{\partial \chi}{\partial T} + y_0 y_1 \frac{\partial^2 \chi}{\partial T^2} \right) + 2\kappa \omega_0 y_0 \frac{dy_0}{d\xi} \frac{\partial \chi}{\partial T} \right. \\ \left. + \frac{2}{\omega_0} \frac{\partial^2 \chi}{\partial \xi \partial T} + \frac{1}{\omega_0^2} \frac{d\omega_0}{d\xi} \frac{\partial \chi}{\partial T} + 2 \frac{\omega_1}{\omega_0} \frac{\partial^2 \chi}{\partial T^2} \right] = 0 \quad (16)$$

This χ equation can now be solved approximately using regular perturbations. We expand χ into an asymptotic series

$$\chi = \chi_0(\xi, T) + \varepsilon \chi_1(\xi, T) + \dots$$

Substituting this into Eq. (16), and collecting terms of the same order, we obtain

$$O(1) : \frac{\partial^2 \chi_0}{\partial T^2} + \chi_0 = 0 \quad (17)$$

$$O(\varepsilon) : \frac{\partial^2 \chi_1}{\partial T^2} + \chi_1 = -2\kappa \omega_0^2 \left(y_0 \frac{\partial y_1}{\partial T} \frac{\partial \chi_0}{\partial T} + y_0 y_1 \frac{\partial^2 \chi_0}{\partial T^2} \right) - 2\kappa \omega_0 y_0 \frac{dy_0}{d\xi} \frac{\partial \chi_0}{\partial T} \\ - \frac{2}{\omega_0} \frac{\partial^2 \chi_0}{\partial \xi \partial T} - \frac{1}{\omega_0^2} \frac{d\omega_0}{d\xi} \frac{\partial \chi_0}{\partial T} - 2 \frac{\omega_1}{\omega_0} \frac{\partial^2 \chi_0}{\partial T^2} \quad (18)$$

Solving Eq. (17) for χ_0 , we get

$$\chi_0 = X(\xi) \cos T \quad (19)$$

From Appendix B, we have the following expression for y_1 :

$$y_1 = \frac{1}{8} y_0 X^2 \cos 2T$$

We substitute this, along with Eq. (19), into Eq. (18) which becomes

$$\frac{\partial^2 \chi_1}{\partial T^2} + \chi_1 = -2\kappa \omega_0^2 \left(\frac{1}{4} y_0^2 X^3 \sin 2T \sin T - \frac{1}{8} y_0^2 X^3 \cos 2T \cos T \right) \\ + 2\kappa \omega_0 y_0 \frac{dy_0}{d\xi} X \sin T + \frac{2}{\omega_0} \frac{dX}{d\xi} \sin T \\ + \frac{1}{\omega_0^2} \frac{d\omega_0}{d\xi} X \sin T + 2 \frac{\omega_1}{\omega_0} X \cos T$$

We make use of the following trigonometric identities:

$$\sin 2T \sin T = \frac{1}{2} \cos T - \frac{1}{2} \cos 3T, \quad \cos 2T \cos T = \frac{1}{2} \cos T + \frac{1}{2} \cos 3T$$

Then, eliminating secular terms from the χ_1 equation results in an expression for ω_1 as well as an equation governing X

$$\omega_1(\xi) = \frac{\kappa}{16} y_0^2 X^2 \omega_0^3 \quad (20)$$

$$\frac{2}{\omega_0} \frac{dX}{d\xi} + \frac{X}{\omega_0^2} \frac{d\omega_0}{d\xi} + 2\kappa \omega_0 y_0 \frac{dy_0}{d\xi} X = 0 \quad (21)$$

We rearrange Eq. (21) into

$$\frac{2}{X} \frac{dX}{d\xi} + \frac{1}{\omega_0} \frac{d\omega_0}{d\xi} + 2\kappa \omega_0^2 y_0 \frac{dy_0}{d\xi} = 0 \quad (22)$$

Recall from Eq. (15) that ω_0 is chosen to be

$$\omega_0 = (1 + \kappa y_0^2)^{-1/2}$$

Then, integrating Eq. (22) with respect to ξ , gives

$$2 \ln X + \ln \omega_0 + \ln(1 + \kappa y_0^2) = k \\ \Rightarrow 2 \ln X + \ln \omega_0 + \ln(\omega_0^{-2}) = k$$

$$\Rightarrow \ln \left(\frac{X^2}{\omega_0} \right) = k$$

$$\Rightarrow X(\xi) = C \sqrt{\omega_0(\xi)} \quad (23)$$

where C is an arbitrary constant that depends on initial conditions. Hence, to leading order, χ takes the following form:

$$\chi \approx C \sqrt{\omega_0(\xi)} \cos T \quad (24)$$

Appendix B. The DPM solution for the slow degree of freedom

The assumed solution has the form:

$$\chi = \chi(\xi, T), \quad y = y_0(\xi) + \varepsilon y_1(\xi, T)$$

where $\xi = t$ and $\frac{dT}{d\xi} = \frac{\omega(\xi)}{\varepsilon}$, $\omega(\xi) = \omega_0(\xi) + \varepsilon \omega_1(\xi) + \dots$

After substituting this into Eq. (3), the equation governing the slow degree of freedom becomes

$$\frac{1}{\varepsilon} \left[\omega_0^2 \frac{\partial^2 y_1}{\partial T^2} - y_0 \omega_0^2 \left(\frac{\partial \chi}{\partial T} \right)^2 \right] + \frac{d^2 y_0}{d\xi^2} + y_0 - 2y_0 \omega_0 \left[\frac{\partial \chi}{\partial \xi} \frac{\partial \chi}{\partial T} + \omega_1 \left(\frac{\partial \chi}{\partial T} \right)^2 \right] \\ - \omega_0^2 y_1 \left(\frac{\partial \chi}{\partial T} \right)^2 + 2\omega_0 \frac{\partial^2 y_1}{\partial \xi \partial T} + \frac{d\omega_0}{d\xi} \frac{\partial y_1}{\partial T} + 2\omega_0 \omega_1 \frac{\partial^2 y_1}{\partial T^2} = 0 \quad (25)$$

From Appendix A, we have that $\chi \approx \chi_0 = X(t) \cos T$. Substituting this into Eq. (25) and expanding the various trigonometric terms, we get

$$\frac{1}{\varepsilon} \left[\omega_0^2 \frac{\partial^2 y_1}{\partial T^2} - y_0 \omega_0^2 X^2 \left(\frac{1}{2} - \frac{1}{2} \cos 2T \right) \right] \\ + \frac{d^2 y_0}{d\xi^2} + y_0 - 2y_0 \omega_0 \left[-\frac{dX}{d\xi} \frac{1}{2} \sin 2T + \omega_1 X^2 \left(\frac{1}{2} - \frac{1}{2} \cos 2T \right) \right] \\ - \omega_0^2 y_1 X^2 \left(\frac{1}{2} - \frac{1}{2} \cos 2T \right) - 2\omega_0 \frac{dX}{d\xi} \sin T \\ + \frac{d\omega_0}{d\xi} \frac{\partial y_1}{\partial T} + 2\omega_0 \omega_1 \frac{\partial^2 y_1}{\partial T^2} = 0 \quad (26)$$

Now, we are ready to carry out the standard steps of the method of direct partition of motion. First, we average Eq. (26) over the fast timescale T , with the assumption that the fast component of motion, y_1 , and its derivatives are periodic on this fast timescale with a zero average. DPM also assumes that any purely slow function, that does not vary on the fast T timescale, is invariant under averaging over fast time. The resulting averaged

equation is

$$\frac{1}{\varepsilon} \left[-\frac{1}{2} y_0 \omega_0^2 X^2 \right] + \frac{d^2 y_0}{d\xi^2} + y_0 - y_0 \omega_0 \omega_1 X^2 + \frac{1}{2} \omega_0^2 X^2 \langle y_1 \cos 2T \rangle_T = 0$$

where $\langle \bullet \rangle_T = \frac{1}{2\pi} \int_0^{2\pi} (\bullet) dT$ (27)

The second standard step of DPM is to subtract Eq. (27) from Eq. (26), then the resulting equation takes the form

$$\frac{1}{\varepsilon} \left[\omega_0^2 \frac{\partial^2 y_1}{\partial T^2} + \frac{1}{2} y_0 \omega_0^2 X^2 \cos 2T \right] + O(1) = 0$$

Hence, to leading order, the equation governing y_1 becomes

$$\frac{\partial^2 y_1}{\partial T^2} + \frac{1}{2} y_0 X^2 \cos 2T = 0$$

Integrating twice with respect to T , we obtain the following expression for y_1 :

$$y_1 \approx \frac{1}{8} y_0 X^2 \cos 2T$$
 (28)

Note that we have set the constants of integration to zero in order to satisfy the DPM assumption that the fast component, y_1 , is periodic on the T timescale with a zero average.

Now, the integral appearing in Eq. (27) can be evaluated as

$$\langle y_1 \cos 2T \rangle_T \approx \left\langle \frac{1}{8} y_0 X^2 \cos^2 2T \right\rangle_T = \frac{1}{16} y_0 X^2$$

Substituting this into Eq. (27), we obtain the following approximate equation governing y_0 :

$$\frac{d^2 y_0}{d\xi^2} + y_0 - y_0 \left(\frac{1}{2\varepsilon} \omega_0^2 X^2 + \omega_0 \omega_1 X^2 - \frac{1}{32} \omega_0^2 X^4 \right) = 0$$
 (29)

From Appendix A, we recall that

$$\omega_1(\xi) = \frac{\kappa}{16} y_0^2 X^2 \omega_0^3 \quad \text{and} \quad X(\xi) = C \sqrt{\omega_0(\xi)}$$

where $\omega_0 = (1 + \kappa y_0^2)^{-1/2}$

Substituting these expressions into Eq. (29), the y_0 equation becomes

$$\frac{d^2 y_0}{d\xi^2} + y_0 - y_0 \left(\frac{C^2}{2\varepsilon} (1 + \kappa y_0^2)^{-3/2} + \frac{\kappa C^4}{16} y_0^2 (1 + \kappa y_0^2)^{-3} - \frac{C^4}{32} (1 + \kappa y_0^2)^{-2} \right) = 0$$
 (30)

where C is an arbitrary constant that depends on the initial conditions. Comparing the magnitude of the denominators of the non-linear terms in the above equation, we expect the first non-linear term to be the dominant one. Hence, for simplification of the required

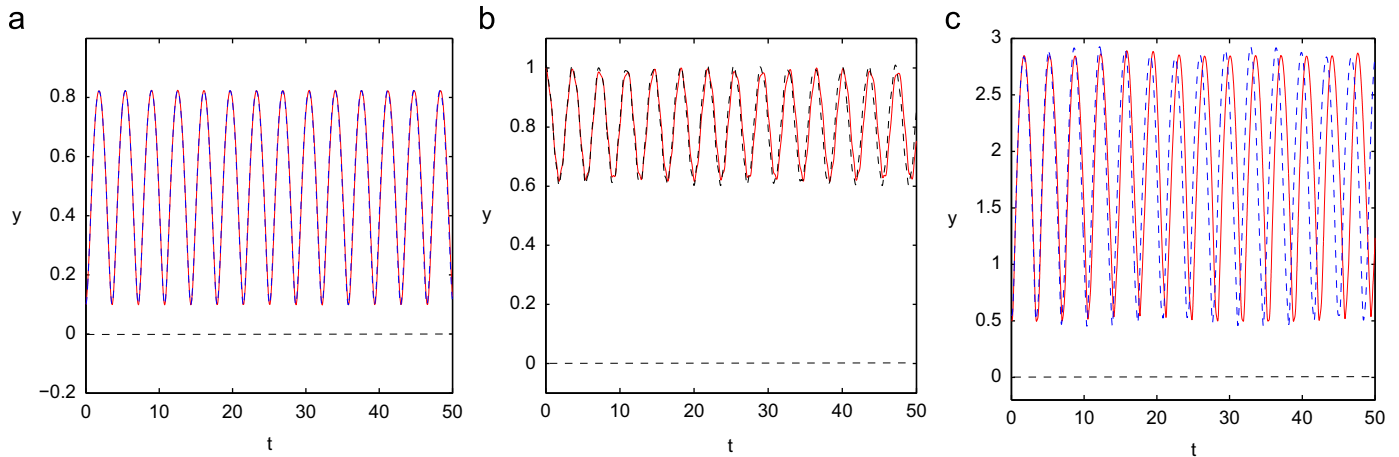


Fig. 11. y vs. time for (a) $h=0.4, b=0.1$, (b) $h=1, b=1$ and (c) $h=5, b=0.5$.

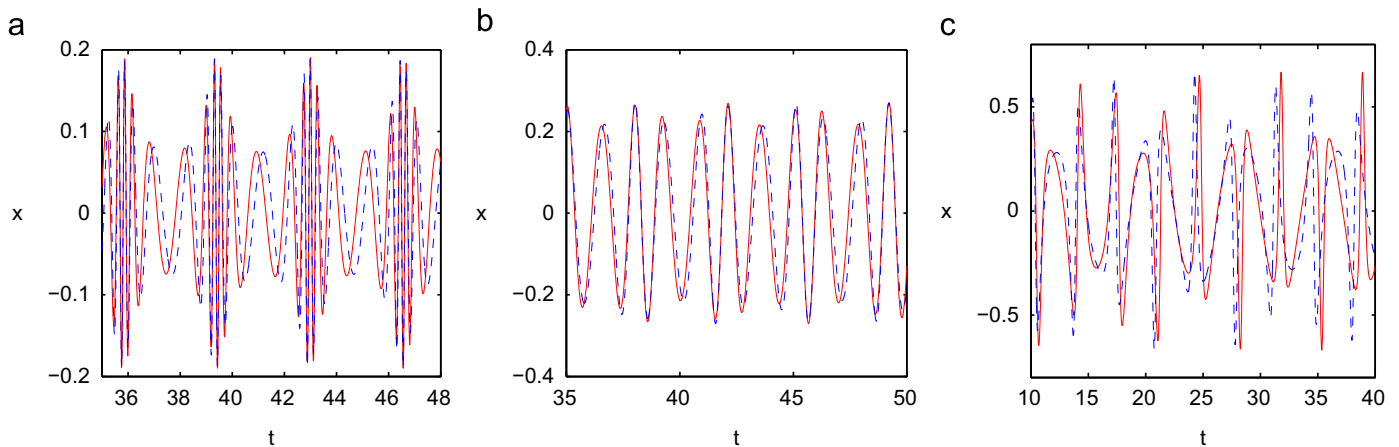


Fig. 12. x vs. time for (a) $h=0.4, b=0.1$, (b) $h=1, b=1$ (c) and $h=5, b=0.5$.

algebraic manipulation, we will ignore the last two terms in the equation. Consequently, y_0 is, to leading order, governed by the following reduced equation:

$$\frac{d^2 y_0}{d\xi^2} + y_0 - y_0 \frac{C^2}{2\varepsilon} (1 + \kappa y_0^2)^{-3/2} = 0 \quad (31)$$

To find an expression for C , we consider initial conditions with zero velocities and initial amplitudes a and b as follows:

$$\begin{cases} y(0) = b \\ x(0) = \chi(0) \sqrt{\frac{\varepsilon}{\gamma}} = a \sqrt{\frac{\varepsilon}{\gamma}} \end{cases} \rightarrow \begin{cases} y_0(0) = b \\ \chi_0(0) = a \end{cases}$$

recalling that

$$\chi_0 = C \sqrt{\omega_0} \cos T \quad \text{where } \omega_0 = (1 + \kappa y_0^2)^{-1/2}$$

then

$$\begin{aligned} \chi_0(0) &= C(1 + \kappa(y_0(0))^2)^{-1/4} \Rightarrow a = C(1 + \kappa b^2)^{-1/4} \\ \Rightarrow C^2 &= a^2 \sqrt{1 + \kappa b^2} \end{aligned} \quad (32)$$

Appendix C. The slow dynamics bifurcation

We restate here the equation governing the leading order dynamics of the slow degree of freedom

$$\frac{d^2 y_0}{d\xi^2} + y_0 - y_0 \frac{C^2}{2\varepsilon} (1 + \kappa y_0^2)^{-3/2} = 0$$

We rewrite this equation as a system of two first order differential equations

$$\dot{y}_0 = \phi, \quad \dot{\phi} = -y_0 + y_0 \frac{C^2}{2\varepsilon} (1 + \kappa y_0^2)^{-3/2} \quad (33)$$

The system in Eq. (33) could possess nontrivial equilibrium points corresponding to $\phi = 0, y_0 = E$, such that E satisfies the following relation:

$$\begin{aligned} 1 - \frac{C^2}{2\varepsilon} (1 + \kappa E^2)^{-3/2} &= 0 \\ \Rightarrow 2\varepsilon(1 + \kappa E^2)^{3/2} &= C^2 \end{aligned}$$

plugging in the expression for C from Eq. (32), we obtain the following relation between E , the value of y_0 for the nontrivial equilibrium point, and the initial amplitudes a and b

$$\Rightarrow 2\varepsilon(1 + \kappa E^2)^{3/2} = a^2 \sqrt{1 + \kappa b^2}$$

the initial condition that corresponds to the bifurcating non-local modes, i.e. fixed points in the Poincare map, will be $y_0(0) = b^*$ such that $E = b^*$, then b^* has to satisfy the following relation:

$$\begin{aligned} 2\varepsilon(1 + \kappa b^{*2})^{3/2} &= a^2 \sqrt{1 + \kappa b^{*2}} \\ \Rightarrow 2\varepsilon(1 + \kappa b^{*2}) &= a^2 \end{aligned} \quad (34)$$

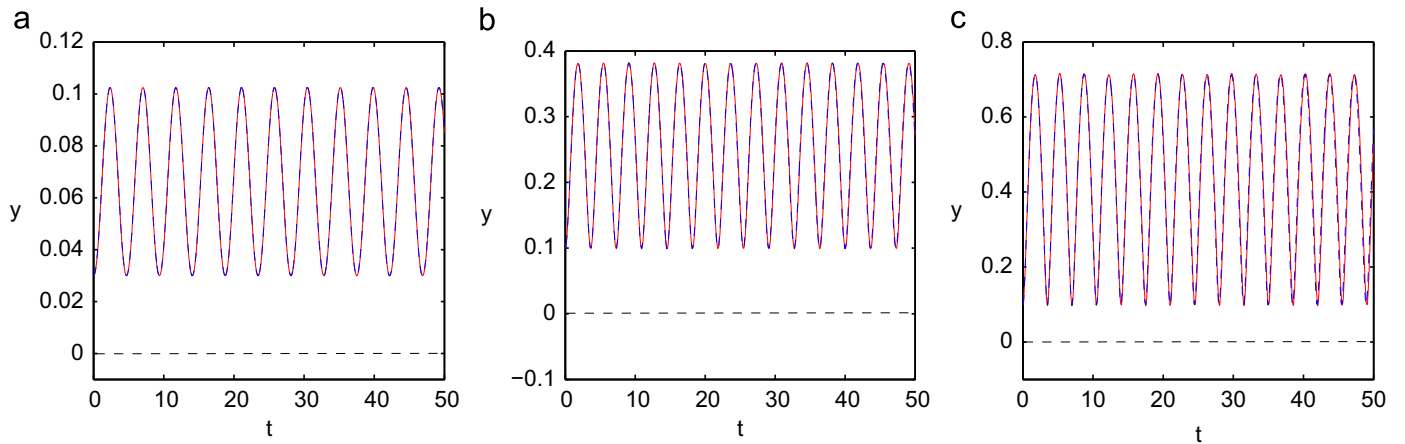


Fig. 13. y vs. time for (a) $h=0.01, b=0.03$, (b) $h=0.1, b=0.1$ and (c) $h=0.3, b=0.1$; with $\gamma=5$.

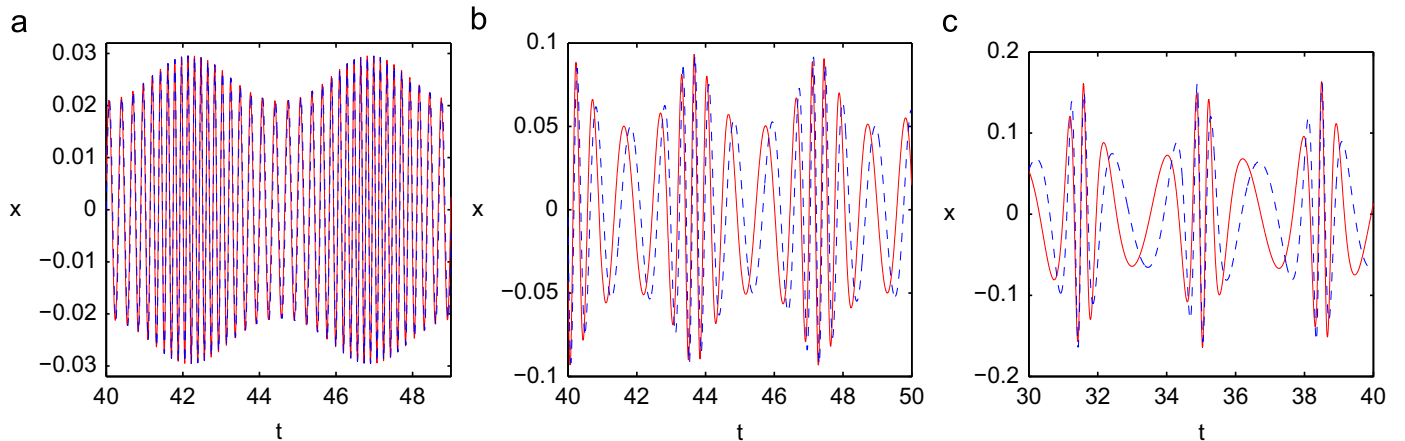


Fig. 14. x vs. time for (a) $h=0.01, b=0.03$, (b) $h=0.1, b=0.1$ and (c) $h=0.3, b=0.1$; with $\gamma=5$.

For such initial conditions with zero velocities, the energy, as given by Eq. (4), reduces to

$$h = \frac{1}{2} \left(\frac{1}{\varepsilon\kappa} a^2 + b^{*2} \right)$$

$$\Rightarrow a^2 = (2h - b^{*2})\varepsilon\kappa$$

plugging this expression for a into Eq. (34), we get

$$\Rightarrow 2\varepsilon(1 + \kappa b^{*2}) = (2h - b^{*2})\varepsilon\kappa$$

$$\Rightarrow b^* = \sqrt{\frac{2}{3} \left(h - \frac{1}{\kappa} \right)} \quad (35)$$

Such special initial conditions will exist when the energy satisfies the following condition:

$$h > h_{cr} = \frac{1}{\kappa} \quad (36)$$

Appendix D. Validation plots for different parameter and energy values

We show more comparison plots for different initial conditions (Figs. 11–14). The parameter values are the same as specified in Section 2, except in Figs. 13 and 14 in which γ is set to 5 instead of 1.74.

References

- [1] I.I. Blekhman, *Vibrational Mechanics: Nonlinear Dynamic Effects, General Approach, Application*, World Scientific, Singapore, 2000.
- [2] J.P. Cusumano, F.C. Moon, Chaotic non-planar vibrations of the thin elastica, part I: experimental observation of planar instability, *Journal of Sound Vibration* 179 (2) (1995) 185–208.
- [3] J.P. Cusumano, F.C. Moon, Chaotic non-planar vibrations of the thin elastica, part II: derivation and analysis of a low-dimensional model, *Journal of Sound Vibration* 179 (2) (1995) 209–226.
- [4] J.S. Jensen, *Non-Trivial Effects of Fast Harmonic Excitation*, Ph.D. Dissertation, DCAMM Report, S83, Dept. Solid Mechanics, Technical University of Denmark, 1999.
- [5] A.H. Nayfeh, C.M. Chin, Nonlinear interactions in a parametrically excited system with widely spaced frequencies, *Nonlinear Dynamics* 7 (1995) 195–216.
- [6] C.H. Pak, R.H. Rand, F.C. Moon, Free vibrations of a thin elastica by normal modes, *Nonlinear Dynamics* 3 (1992) 347–364.
- [7] H. Sheheitli, R.H. Rand, Dynamics of three coupled limit cycle oscillators with vastly different frequencies, *Nonlinear Dynamics* 64 (2011) 131–145.
- [8] H. Sheheitli, R.H. Rand, Dynamics of a mass-spring-pendulum system with vastly different frequencies, to appear.
- [9] J.J. Thomsen, *Vibrations and Stability, Advanced Theory, Analysis and Tools*, Springer-Verlag, Berlin, Heidelberg, Germany, 2003.
- [10] J.J. Thomsen, Slow high-frequency effects in mechanics: problems, solutions, potentials, *International Journal of Bifurcation Chaos* 15 (2005) 2799–2818.
- [11] J.M. Tuwankotta, F. Verhulst, Hamiltonian systems with widely separated frequencies, *Nonlinearity* 16 (2003) 689–706.
- [12] D.C. Wilcox, *Perturbation Methods in the Computer Age*, DCW Industries Inc., CA, 1995.